

Oblique evaporation of $\text{Co}_{80}\text{Ni}_{20}$ part II: continuously varying angle of vapour incidence

Peter TEN BERGE¹, Leon ABELMANN¹, Cock LODDER¹, Ab SCHRADER², Steven LUITJENS²

¹MESA Research Institute, University of Twente, PO Box 217, 7500 AE Enschede, The Netherlands

²Philips Research Laboratories, Magn.Rec. Dept., PO Box 80000, 5600 JA Eindhoven, The Netherlands

Abstract--- A mini-rollcoater deposition system has been built in order to prepare metal evaporated tapes. The deposition rate of the $\text{Co}_{80}\text{Ni}_{20}$ was varied. It appears that the value of the coercivity can partly be explained by considering the effect of oxidation on the diffusion processes. The inclination of the columns depends on the deposition rate and the oxygen supply. Low temperature hystereses showed a large ferromagnetic-antiferromagnetic coupling effect. Recording experiments show that a high coercivity is necessary for acceptable output at high frequencies; intrinsic domains are suggested to limit the smallest recordable wavelength.

INTRODUCTION

Due to their good recording properties, metallic thin films are nowadays in use for magnetic tape recording. It is extremely important that these thin films consist of non-interacting magnetic units, for the sake of a high coercivity and a low medium noise. Therefore it is necessary to exploit laterally inhomogeneous thin films, whether in composition or in structure.

In several studies about the oblique evaporation of $\text{Co}_{80}\text{Ni}_{20}$ under a fixed angle [ref.1-3] models are suggested that show how the coercivity, the anisotropy in longitudinal and transversal direction, the magnetic easy axis and the remanence vary with deposition conditions such as rate, oxidation degree and incidence angle. Although direct extrapolation of these models to continuously deposited Co-Ni-O films is not possible, they may be used for the interpretation of their properties. Several major differences in deposition conditions object to a direct extrapolation, e.g. the base film is in most cases a polyester-type polymer with added fillers, the incidence angle is continuously varying (from grazing incidence to 30-50° with the normal) and the oxygen is supplied at a localized position. These aspects result in a different structure of the continuously deposited Co-Ni-O films compared to fixed angle films.

The resulting morphology of the continuously deposited films is generally believed to consist of fibers (< 10 nm) and bundles of fibers (columns) with some separation between the fibers; the fibers consist of ferro- and non-magnetic grains. The films do not seem to be totally crystalline, but partly amorphous and several oxide and metallic phases have been observed [ref.4]. The oxygen addition leads to an increased oxide concentration at the top of the films, and in fact serves several goals: besides the increased efficiency of the deposition process due to O_2 addition, the surface has a higher corrosion resistance.

In high density recording for digital video storage purposes, the need for a bit area of about $1 \mu\text{m}^2$ is anticipated [ref.5]. From thermal activation measurements an intrinsic switching volume of about 2300 nm^3 is

inferred [ref.6]; this means that -for a 150 nm thick 60% density film- $3.9 \cdot 10^4$ magnetic units are present in one bit. This number is an important factor determining the signal to noise ratio. By optimizing the interactions between the grains, fibers and/or columns and their origins as a function of the deposition process, the size of the smallest magnetic units can be tailored. In this way smaller bit sizes might become available in a recording system using metal evaporated tape. In this paper we report on the properties of Co-Ni-O films, prepared by a mini-rollcoater system, with emphasis on their large-scale magnetic behaviour and their microstructure in relation with their recording behaviour.

EXPERIMENTAL

The mini-rollcoater has been built into a Leybold Heraeus L560 e-beam evaporation system [1] and consists of a solid drum with the 11 μm PET base film (Toray Q68S) stretched around it (see figure 1). A $\text{Co}_{80}\text{Ni}_{20}$ source is heated by an e-beam with a trajectory over the crucible such that a high evaporation rate is possible (up to 30 nm/s at 0°); the vapour flux is inhibited by a shield with a variable opening, thus defining the desired angle range of incidence of 90° down to 60°. The oxygen supply is located at the 60° angle of incidence side. The pressure during deposition is in the order of $5 \cdot 10^{-6}$ mbar.

Prior to a deposition cycle, the base film is reactively cleaned by a glow discharge treatment. The deposition rate and the revolution time of the drum are variable. The process conditions in the mini-rollcoater are approaching those used in industrial applications, apart from the deposition rate, which is lower. Since the oxygen flow is very much system-dependent, we discriminate between high (4.3 sccm), medium (2.1 sccm) and no oxygen flow; here, we only show the high oxygen flow series. From the metal evaporated tape (total $\pm 200 \text{ cm}^2$) samples are taken for magnetic and structural analyses and 8 mm tape is cut for tape recording experiments. Magnetic measurements have been performed on an Oxford Instruments VSM, while the torque magnetometer measurements have been performed on a homebuilt instrument.

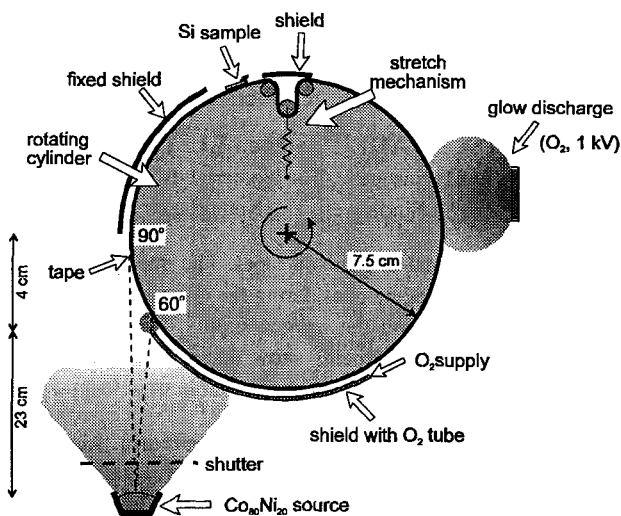


Figure 1. Schematic drawing of the rollcoater.

Temperature-dependent hysteresis loops in the longitudinal direction have been performed by field-cooling through the Neél temperature of CoO at an applied field of 3 Tesla. The rotating drum recording set-up employs a ring head with a gap width of 0.25 μm , a track width of 27 μm and 20 turns. Typical head-to-tape velocity is in between 1.5 and 3 m/s; the output was normalised to 1 m/s. The square wave writing current is optimised for maximum output at 1 μm wavelength. As a lubricant Fomblin Y-25 is used.

RESULTS

In table I we give some deposition and magnetic parameters of the tapes we will discuss hereafter. The subscript *p* (parallel) stands for parallel to the incidence vapour plane. It is noted that the deposition rate to rollcoater revolution ratio, as well as the oxygen flow (4.3 sccm) is kept constant in all deposition cycles.

Table I. Deposition and magnetic parameters of 3 tapes

tape #	rate (nm/s)	δ (nm)	M_S (kA/m)	$H_{c,p}$ (kA/m)	H_K (kA/m)	easy* axis ($^\circ$)
A	21	128	855	34	342	23
B	14	162	348	38	354	34
C	7	200	129	119	394	47

* with respect to film plane, corrected for sheet demagnetisation

Magnetic measurements

In table I the $H_{c,p}$ of tape C is large, considering the values of M_S and H_K ($=2.K_0/\mu_0.M_S$); this may be indicative of a changing coupling mechanism from tapes A-B to C. In figure 2 the parallel hysteresis curves of 3 different tapes are shown. The saturation magnetisation of the loops becomes smaller with decreasing rate; this obviously originates from the oxygen flow. In this oxygen flow series, the coercivity increases with lower deposition rate; this is somewhat unexpected, since for fixed angle oblique evaporation the parallel coercivity becomes

smaller when the rate is decreased, due to a smaller interfiber separation [ref.1,7]. Apparently the oxygen incorporation is of more effect to the coercivity than the deposition rate is. This can be explained by assuming that the reacting oxygen during deposition impairs the random surface diffusion (i.e. less oxygen results in smaller interfiber separation), by a stronger oxidation of the metal columns, or by a distortion of the grain crystalline or morphological structure.

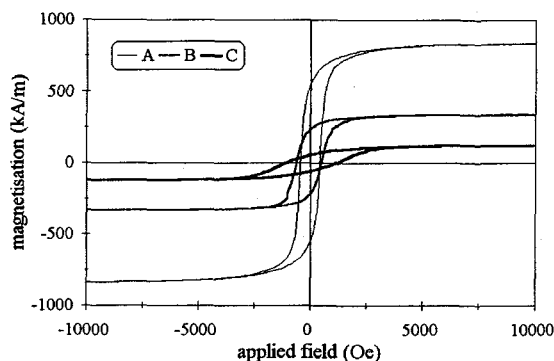
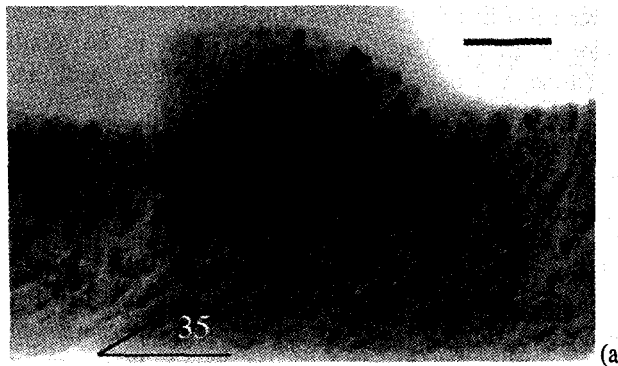


Figure 2. Parallel hystereses of 3 ME tapes.

Morphology

Auger depth profiling showed us that the Co/Ni ratio is constant over the total depth of the tapes. The oxygen concentration is enhanced in the top 30 nm, as a result of the localized oxygen supply, and in the bottom 10 nm, where the effective deposition rate at grazing angle is small. From bright field TEM images of tapes A-C it can be seen that the tilt angle of the columns relative to the substrate becomes larger for the stronger oxidized films (figure 3). This shows how the random surface diffusion is stronger limited by the oxygen at low deposition rates, leading to a columnar growth towards the normal as a result of a larger effect of the conserved momentum of the incoming atoms. From figure 3 it can also be seen that the crystallite size increases with a lower deposition rate and/or higher oxygen incorporation; this is supported by dark field TEM images, showing maximum crystal sizes of about 7, 14 and 22 nm for tapes A,B and C, respectively, taken of the areas in figure 3.



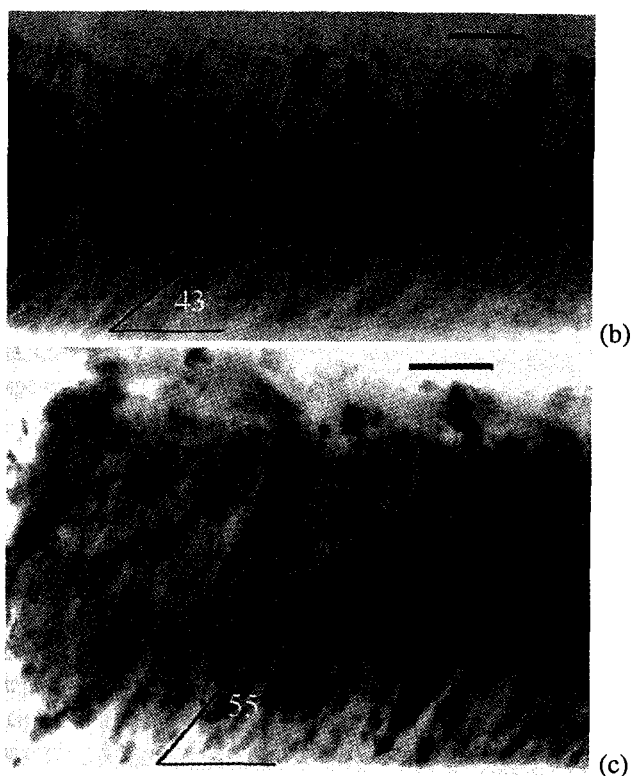


Figure 3. Bright field TEM images of (a) tape A, (b) tape B and (c) tape C; bar = 40 nm.

In table II we give the main diffraction rings, obtained by selected area electron diffraction (taken over the total thickness). From the table it is deduced that CoO and NiO phases are present in all tapes, but that the Co hcp phases are only predominantly present in tape A and Hi8ME. Furthermore, the diffraction rings in tape A and Hi8ME are less sharp, pointing at smaller crystallite sizes as well.

Table II. Main diffraction rings in tapes A-C and Hi8.

crystal phase	A	B	C	Hi8
CoO (111) fcc	x	x	x	x
NiO fcc	x	x	x	x
Co (1011) hcp	x	-	-	x
CoO (220) fcc	x	x	x	x
Co (1110) hcp / CoO(311) fcc	x	x	x	x
Co (1013) hcp / Co (220) fcc	x	-	-	-
Co (1112) hcp / Co (311) fcc	x	x	x	x

In order to learn more about the oxidized state of our tapes, we cooled them from 295 to 40 Kelvin under application of an external field of 3 Tesla. Under these circumstances, a *unidirectional* contribution to the anisotropy can be measured [ref.8]. The antiferromagnetic oxide phase aligns to the saturated ferromagnetic phase. Cooling down through the Neel temperature ($T_{Neel}(CoO) = 293$ K) will cause a decrease in the susceptibility of the antiferromagnetic phase, and at 40 Kelvin it does hardly respond to an external applied field. Reversal of the applied field (i.e. measuring a hysteresis) will be counteracted if exchange coupling is present between the Co and

CoO and the contact area between the Co phase on one side and the CoO on the other side is close enough.

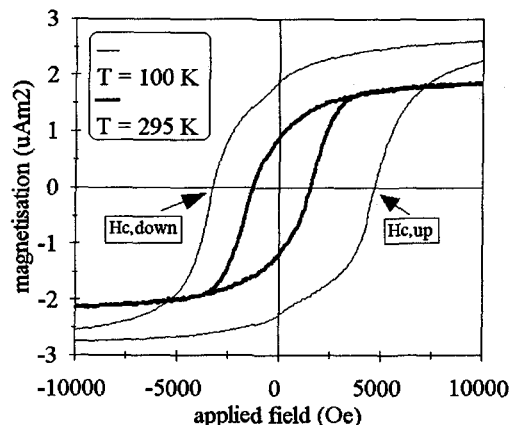


Figure 4. In-plane hysteresis loops (enlarged) of tape C at 100 and 295 K, showing exchange coupling.

Practically, this results in a shift of the total hysteresis loop (see figure 4). If we compare the shift of the hysteresis loops of tapes A-C and that of a commercial Hi8ME tape, it is seen that this shift is not the same for all tapes. This is shown in figure 5, where ΔH_C denotes the shift of the hysteresis expressed as $|H_{C,up} - H_{C,down}|$ in kA/m as a function of the measurement temperature.

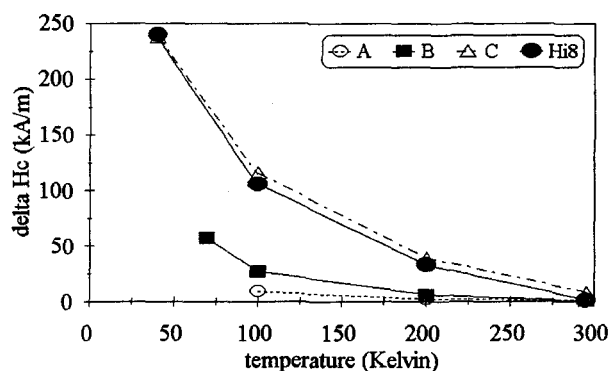


Figure 5. Hysteresis shift ΔH_C vs. meas. temperature.

It is clear from the figure that the exchange coupling at low temperatures is predominantly present for tape C and Hi8, and becomes smaller for B and A. Although the shift is equal for C and Hi8, the oxidation of the tapes must be different: the saturation magnetisation of tape C is 3 times smaller than that of Hi8 with equal thickness, pointing at a stronger oxidized tape C. Assuming the contact area between the Co and CoO phases proportional with the shift of the loops, we suggest that tape C consists of grains with thicker oxide shells. The ferromagnetic Co cores of the grains in tape C are thus decoupled; this may explain the very high in-plane coercivity of C (119 kA/m). A decoupling effect in tape C is supported by the low in-plane coercivities of tapes A-B and the relatively low deposition rate (see table I), combined with the lower

hysteresis shift in figure 5. The high in-plane coercivity of Hi8 (97 kA/m) can, apart from oxidation effects, be explained the high deposition rate (100-200 nm/s), resulting in a larger interfiber separation.

Recording

In figure 6 the normalised frequency spectra of tapes A-C are shown, together with that of Hi8ME tape.

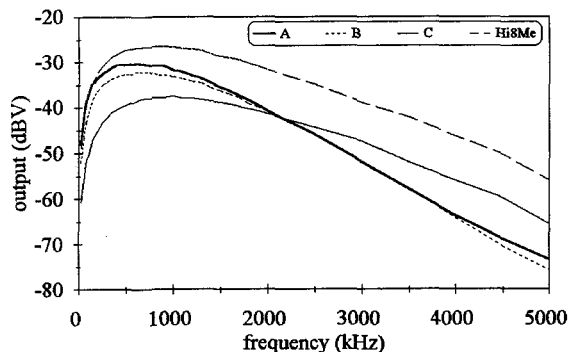


Figure 6. Frequency spectra of tapes A-C and Hi8ME.

The smaller slope at high frequencies for tapes C and Hi8ME shows us the effect of a high coercivity, resulting in a small transition zone. The smaller output of tape C as a whole and especially at low frequencies can be accounted for by a low value of the M_r . The oxidized surface layer of tape C (and its high H_c) was also reflected by the very high write current necessary to optimise the output.

In figure 7 the MFM images are shown of tapes C and Hi8ME. For both tapes it was not possible to reproduce higher frequencies, while the smallest wavelength reproduced by MFM for tapes A and B was 1 μm . Possibly the presence of the intrinsic domains in figure 7 (see arrows), being of the minimum wavelength size, can account for this.

CONCLUSIONS

The metal evaporated tapes prepared in our mini-rollcoater have been characterised considering the deposition rate and oxygen incorporation; the effect of these parameters on the coercivity can be explained in terms of surface diffusion and the resulting decoupling of the grains by interfiber separation and / or oxidation. A large ferromagnetic-antiferromagnetic coupling effect is shown for these tapes by measuring low temperature hystereses. The inclination of the columns and the grain sizes are seen to depend on the ratio deposition rate to oxygen supply. Recording experiments show that a high coercivity is necessary to obtain acceptable output at high frequencies, while the remanence value (M_r) becomes more important at low frequencies. MFM images of the highest reproducible frequencies show intrinsic domains of the wavelength size, possibly determining the smallest recordable wavelength.

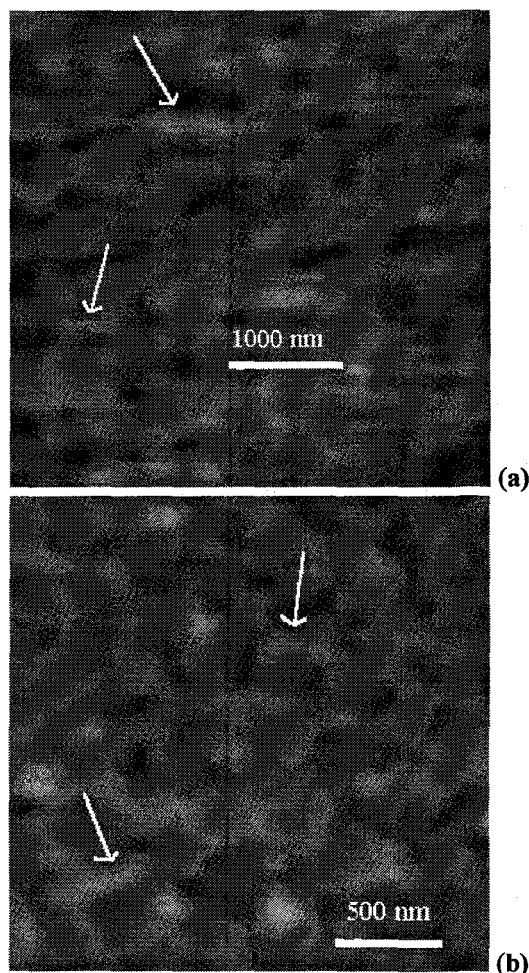


Figure 7. MFM images of (a) 0.5 μm period signal in tape C and of (b) 0.25 μm period signal in Hi8ME.

ACKNOWLEDGEMENT

Dr. M. Rührig is acknowledged for MFM measurements. This project is supported by CAMST.

REFERENCES

1. L. Abelmann *et al.*, Oblique evaporation of $\text{Co}_{80}\text{Ni}_{20}$ part I: Fixed angle of vapour incidence, proceedings PMRC 1994.
2. H. Ho *et al.*, Domain structure and microstructure of CoNi oblique incidence thin films, J.A.P. 65(8) p.3161-6 (1989).
3. K. Hara *et al.*, Magnetic anisotropy of obliquely vapor-deposited CoNi films, J.M.M.M.. 102 pp.247-54 (1991).
4. G. Krijnen *et al.*, Correlation between anisotropy direction and puls shape for metal evaporated tape, IEEE Trans.Magn. 24(2) pp.1817-9 (1988).
5. S.B.Luitjens, Magnetic recording trends: media development and future (video) recording systems, IEEE Trans.Magn. 24 (6) pp 6-11 (1990).
6. H.J.Richter, An analysis of magnetization processes in metal evaporated tape, IEEE Trans.Magn. 29(1) pp.21-33 (1993).
7. K.Hara *et al.*, Oblique-incidence anisotropy of the iron films evaporated at low substrate temperature, JMMM. 73 pp.161-6 (1988).
8. W.Meiklejohn *et al.*, New magnetic anisotropy, Phys.Rev. 105 pp.904-13 (1957).